J|A|C|S COMMUNICATIONS

Published on Web 07/02/2010

INEPT-Based Separated-Local-Field NMR Spectroscopy: A Unique Approach To Elucidate Side-Chain Dynamics of Membrane-Associated Proteins

Jiadi Xu,[†] Ronald Soong,[†] Sang-Choul Im,[‡] Lucy Waskell,[‡] and Ayyalusamy Ramamoorthy*,[†]

Biophysics and Department of Chemistry, University of Michigan, Ann Arbor, Michigan 48109-1055, and Department of Anesthesiology, University of Michigan, and VA Medical Center, Ann Arbor, Michigan 48105

Received May 10, 2010; E-mail: ramamoor@umich.edu

Abstract: Despite recent advances in NMR approaches for structural biology, determination of membrane protein dynamics in its native environment continues to be a monumental challenge, as most NMR structural studies of membrane proteins are commonly carried out either in micelles or in vesicle systems under frozen conditions. To overcome this difficulty, we propose a solid-state NMR technique that allows for the determination of side-chain dynamics from membrane proteins in lipid bilayers. This new technique, namely dipolar enhanced polarization transfer (DREPT), allows for a wide range of dipolar couplings to be encoded, providing high resolution and sensitivity for systems that undergo motional averaging such as that of amino acid side chains. NMR observables such as dipolar couplings and chemical shift anisotropy, which are highly sensitive to molecular motions, provide a direct way of probing protein dynamics over a wide range of time scales. Therefore, using an appropriate model, it is possible to determine side-chain dynamics and provide additional information on the topology and function of a membrane protein in its native environment.

Dynamics is crucial to the function of membrane-associated molecules such as peptides and membrane proteins.[1] In particular, the dynamics of amino acid side chains play a central role in the folding and oligomerization of membrane proteins as well as in their functions, including ion transport and cell membrane disruption. Therefore, an amino acid sequence encodes not only the structure of a protein but also a range of accessible dynamics, which in most cases determines its function as well as its adaptability to various stimuli such as temperature, pH, and ionic strength. While solving atomic-level-resolution structures of membrane-associated proteins is a challenge, characterization of their dynamics at high resolution is even more difficult. In particular, measurement of protein dynamics from physiologically relevant fluid membranes is a major challenge, as solid-state NMR structural studies of membrane proteins are commonly carried out using frozen model membranes such as multilamellar vesicles.[2−4]

To overcome these limitations, we propose a 2D solid-state NMR technique that allows the determination of side-chain dynamics from a membrane protein in its near-native environment. This technique, namely dipolar-enhanced polarization transfer (DREPT), is a hybrid of proton-evolved local field (PELF)[6] and refocused insensitive nuclei enhanced by polarization transfer (INEPT) techniques.[7] The schematic of the radio frequency (RF) pulse sequence is given in Figure S1 (Supporting Information). A homonuclear dipolar-decoupling pulse sequence is inserted in the delay periods of the refocused-INEPT (RINEPT) pulse sequence, allowing for the proton transverse magnetization to evolve under heteronuclear (scaled-dipolar and scalar) couplings during the incrementable t_1 period. The efficiency of this technique is demonstrated using magnetically aligned fluid lamellar-phase bicelles containing a 16.3 kDa mutant cytochrome-b_5 (Cyt-b_5), a heme-containing membrane-anchored protein.[8] The amino acid sequences of wild-type and mutant Cyt-b_5 are given in Figure S2 (Supporting Information). As shown in our previous study,[9] this protein exhibits dynamics covering a wide range of time scales (nanoseconds to milliseconds) and therefore is an excellent system to examine the efficiency of the DREPT pulse sequence to selectively measure the dynamics of amino acid side chains in fluid lamellar-phase lipid bilayers. Since the time period required to refocus the antiphase ^{15}N magnetization is highly sensitive to the magnitude of the NH dipolar coupling, which depends on the mobility of the associated amino acid residue, spectral editing can be performed based on the dynamics of different segments of the protein, as demonstrated in Figure 1. For example, a short delay of 60 μs is sufficient to refocus the antiphase ^{15}N magnetization from residues in the transmembrane domain of the protein due to their large NH dipolar couplings ($\sim$3$-$5 kHz).[9,10] On the other hand, due to the fast time scale of motion for residues in the soluble domain, their resonances only appear in the spectra collected with longer refocusing delays. Spectra obtained from the DREPT pulse sequence are compared with those obtained from RINEPT and ramp cross-polymerization (CP) in Figure 1. Our results suggest that the DREPT pulse sequence provides a better spectral sensitivity than the RINEPT pulse sequence. This is a direct consequence of the loss of proton transverse magnetization due to ^{1}H$-^1$H dipolar interactions during the delay periods in the RINEPT pulse sequence, which are avoided in the DREPT pulse sequence by applying a windowless homonuclear dipolar decoupling multiple-pulse sequence, namely BLEW.[11] Therefore, the one-dimensional version of the DREPT pulse sequence can be used for spectral editing based on dynamical differences between different segments of a membrane protein. Interestingly, the signal intensity of resonances originating from the soluble domain of the mutant Cyt-b_5 is significantly higher in the DREPT spectra compared to those obtained using ramp-CP[12] with a contact time comparable to the refocusing delay of DREPT. This reflects the difference in the magnetization transfer efficiency between the two techniques. A broad time scale of dynamics associated with residues in the soluble domain of the protein attenuates the ramp-CP efficiency. On the other hand, in the DREPT pulse sequence, the transfer of transverse magnetization from abundant proton nuclei to rare X nuclei (^{15}N or ^{13}C) is via a combination of dipolar and J couplings. A defined length of the delay period controls the efficiency of this magnetization transfer. While not all heteronuclear dipolar couplings can be satisfied by a given delay period in the DREPT sequence, a significant amount of magnetization transfer can still occur,

[†] Biophysics and Department of Chemistry.
[‡] Department of Anesthesiology and VA Medical Center.

10.1021/ja103983f

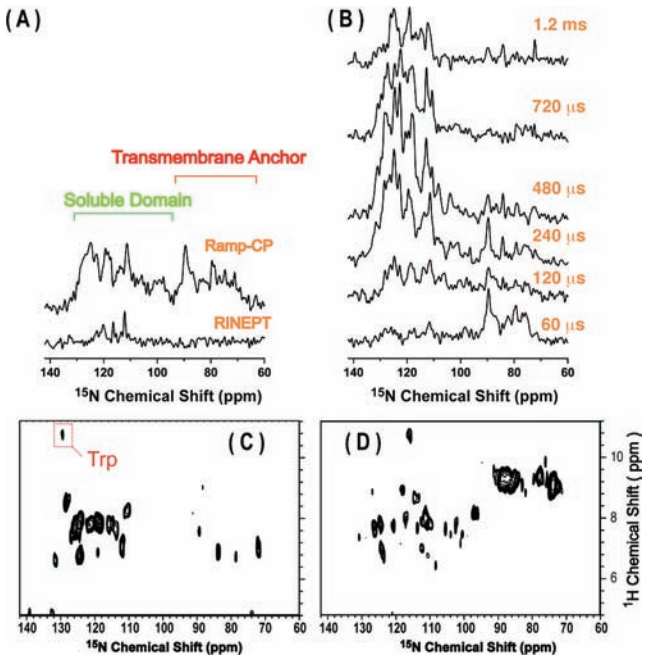

Figure 1. Series of ^{15}N chemical shift spectra acquired using ramp-CP and RINEPT (A) and DREPT (B) experiments on magnetically aligned bicelles containing a uniformly ^{15}N-labeled mutant cytochrome-b_5. The contact time used for ramp-CP was 800 μs. The delay periods used in RINEPT were $\tau_1 = \tau_2 = 2$ ms. The refocusing delay (τ_2) in the DREPT sequence used to obtain each spectrum in (B) is indicated, and in all these cases $\tau_1 = \tau_2$. All the spectra were acquired using 2000 scans and a 3 s recycle delay. (C,D) 2D ^{1}H$-^{15}$N HETCOR spectra of the same sample obtained using the DREPT pulse sequence (Figure S1, Supporting Information). These spectra were acquired using 20 t_1 increments, 800 scans per increment, and a 3 s recycle delay. The τ_2 delay period used in these HETCOR spectra was 1 ms for (C) and 80 μs for (D).

contributing to the overall intensity of the spectrum, as seen in Figure 1. This versatile capability of the DREPT pulse sequence to act as a spectral editing method is of tremendous advantage in identifying the topology of different segments of a membrane protein in lipid bilayers and can also be used for resonance assignment when combined with other approaches. For example, 2D heteronuclear correlation of chemical shifts (HETCOR) spectra obtained using the DREPT pulse sequence are presented in Figures 1C and 1D. By suitably varying the refocusing delay period, different regions of the protein can be selected in the HETCOR spectrum. For example, with a short refocusing delay (τ_2), the HETCOR spectrum showed only the rigid part of the protein, such as the resonances from the transmembrane domain. On the other hand, when a long refocusing delay was used, only the mobile region of the protein was observed in the HETCOR spectrum.

A 2D separated-local-field (SLF) version of the DREPT sequence shown in Figure S1 can be generated using the first delay (τ_1), during which antiphase proton magnetizations are generated, as an incremental t_1 period to measure NH dipolar couplings and to correlate with ^{15}N chemical shift anisotropy (CSA) in the direct dimension. This manner of encoding the NH dipolar coupling is similar to that of the PELF sequence.[10] Therefore, this 2D DREPT method provides high sensitivity and resolution for membrane protein segments that undergo rapid motional averaging and can be utilized in the measurement of NMR parameters pertaining to amino acid side chains by effectively suppressing resonances from immobile regions of the protein, as demonstrated in Figure 2.

Since NMR parameters such as dipolar couplings and CSA are highly sensitive to molecular motion, the DREPT method offers a

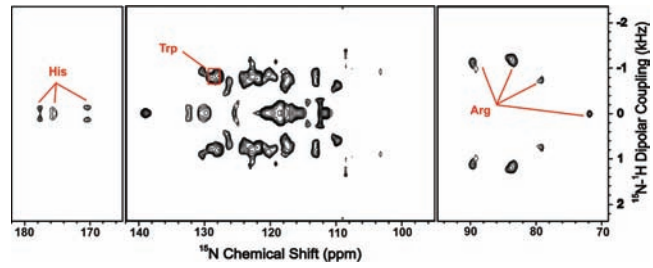

Figure 2. 2D DREPT-SLF spectrum of uniformly ^{15}N-labeled mutant cytochrome b_5 in magnetically aligned bicelles obtained using the pulse sequence given in Figure S1 (Supporting Information) with $\tau_1 = \tau_2 = 400$ μs. In this spectrum, dipolar couplings associated with different type of side chains can be identified. These results suggest that long refocusing delays suppress resonances from rigid parts of the protein (i.e., the transmembrane region) and allow for the identification of resonances and measurement of NH dipolar couplings associated with side chains. Only those regions of the 2D spectrum that contain peaks are shown.

direct means of monitoring protein dynamics covering a wide range of time scales. While a previous solid-state NMR study revealed the dynamical difference between the soluble and transmembrane domains of Cyt-b_5 using backbone resonances, the measurement of side-chain dynamics has not been possible due to poor spectral resolution.[9] To demonstrate the utility of the 2D DREPT method in measuring NH dipolar couplings associated with amino acid side chains, a series of 2D SLF spectra were acquired from magnetically aligned bicelles containing a uniformly ^{15}N-labeled mutant Cyt-b_5. Since the second delay period (τ_2) of the pulse sequence can be tuned to select resonances from specific regions of the spectrum, spectral regions corresponding to the side chains of a protein can be isolated and acquired for dynamical analysis. For instance, resonances at 80 and 90 ppm originate from the side chain of Arg, resonances at 129 and 130 ppm correspond to the side chain of Trp, and resonances from 169 to 177 ppm belong to the His side chain in the soluble domain. (Resonance assignment is shown in Figures 1C, 1D and S3.) However, due to the overlap of resonances, all three Trp residues in the membrane-spanning domain are not resolved. Due to the mobility of these side chains, the observed ^{15}N chemical shift values are nearly equivalent to their isotropic chemical shift values, which facilitate the resonance assignment. Because of the large magnitude of NH dipolar couplings ($\sim$1 kHz) observed for Arg and Trp side chains, these residues are most likely located in the transmembrane region of the protein, where the mobility is relatively restricted and therefore increases the order of amino acid side chains.

Whole-body motions of the helix coupled with side-chain dynamics attenuate the observed dipolar couplings associated with side chains. Thus, the observed NH dipolar couplings from side chains are scaled according to the following equation,

$$D_{\mathrm{obs}} = D_{\mathrm{NH}} S_{\mathrm{H}} S_{\mathrm{SC}} \qquad (1)$$

where D_{NH} is the NH dipolar coupling in the rigid limit, S_{H} is the order parameter of the helix, which for bicelles is estimated to be 0.8 from a previous study,[10] and S_{SC} is the order parameter of a side chain. S_{SC}, therefore, describes the overall motion and fluctuations in the side-chain orientation. Based on the S_{SC} order parameters, it is possible to construct a model that describes the dynamics of amino acid side chains of a protein embedded in lipid bilayers. The S_{SC} order parameter can be decomposed into two components, as given below:

$$S_{\mathrm{SC}} = (1/2) S_{\mathrm{local}} \langle 3 \cos^2 \vartheta - 1 \rangle \qquad (2)$$

Table 1. Summary of Amino Acid Side-Chain Chemical Shifts and Order Parameters Calculated from Experimentally Measured Dipolar Couplings from Magnetically Aligned Bicelles Containing ^{15}N-Labeled Mutant Cyt-b_5

residue	^{15}N chemical shift (ppm)	NH dipolar coupling (kHz)	S_{SC}
Trp	129.7	0.80	0.15
	128.2	0.82	0.17
Arg	90.0	1.13	0.22
	84.2	1.22	0.24
	79.2	0.77	0.14
His[a]	177.7	0.12	0.05
	175.7	0.09	0
	169.9	0.15	0.01

[a] The His residue is in the soluble domain of the protein and exhibits a relatively small degree of order.

where ϑ is the angle between the director axis (d_{sc}) of a side chain and the helical axis (d_H) and S_{local} is the order parameter describing the fluctuation in the orientation of d_{sc}; the term $\langle\cdots\rangle$ denotes an average over the molecular motion, such as bond libration and rotation about the C−C bond in the side chain, which are fast relative to $1/D_{NH}$. Since large fluctuations are possible in a side chain, two models can be used to describe their motion: diffusion in a cone and orientational fluctuations. For the case of fluctuations in the orientation of the director axis of a side chain, the S_{local} order parameter is expressed according to eq 3,

$$S_{local} = (1/2)\langle 3\cos^2\alpha_f - 1\rangle \quad (3)$$

where α_f is the angle between the director axis of fluctuation (d_m) and d_{sc}. If d_m is collinear with d_{sc}, then S_{local} will be equal to 1, which implies minor or negligible fluctuations in d_{sc}. For the case of the "diffusion in a cone" model, the orientation of d_{sc} is described as wobbling inside a cone defined by a semi-cone angle, α_c:[13]

$$S_{local} = (1/2)(\cos\alpha_c)(1 + \cos\alpha_c) \quad (4)$$

In this case, the S_{local} order parameter is expressed according to eq 4. Order parameters calculated from experimentally measured dipolar couplings are summarized in Table 1.

The orientation of various director axes of motions for different types of side chains is shown in Figure 3. Due to the rapid rotation about C−C bonds in Arg, d_{sc} is collinear with the side chain. On the other hand, due to the rigidity of the indole ring in Trp, the observed NH dipolar coupling reflects only the orientation of the N_ε−H bond vector with respect to the helical axis. Since the N_ε−H bond vector is perpendicular to the indole ring normal, it is insensitive to the orientation of the indole ring. While the orientation of the indole ring cannot be deduced solely from the N_ε−H dipolar coupling, its dynamics is certainly encoded in the S_{local} order parameter. Therefore, S_{local} can be used to describe the dynamics of the indole ring. If α_c or α_f is equal to zero, implying a small degree of fluctuation in d_{sc}, both models predict the orientation of the Arg side chain to be 45−47° relative to the helical axis. For the case of Trp, the orientation of the N_ε−H bond vector is estimated to be 50°. Interestingly, based on our simulations shown in Figure S4, only a large fluctuation (α_c or $\alpha_f > 30°$) will change the orientation of side chains. Therefore, ϑ values determined from this study provide an upper limit for side-chain orientations in lipid bilayers. This upper limit value is in agreement with the reported value for the methyl group orientation (~56°) of alanine, which experienced a limited side-chain motion.[14] Thus, our approach

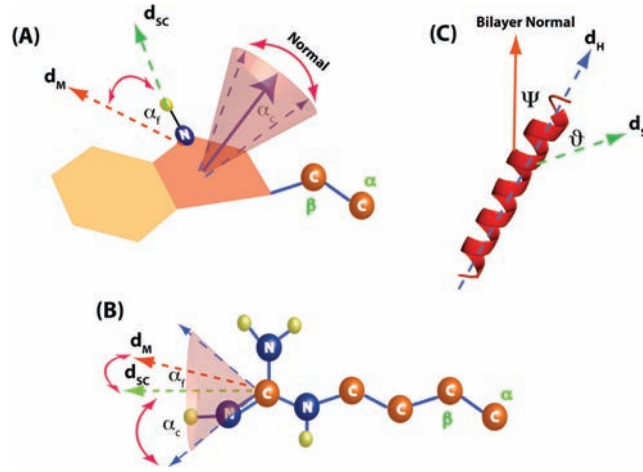

Figure 3. Schematics showing the orientation of the director axes d_M, d_{sc}, and d_H relative to the geometry of the protein and the side chains. The dipolar couplings of the side chains are projected along the d_{sc} director axis due to the rapid internal motions inherent in the side chain, such as bond libration and isomerization, relative to the NMR time scale ($1/D_{NH}$). d_M is the director axis of motions describing the fluctuations of d_{sc}. d_H represents the director axis of the helix. (A) Diagram showing the orientations of d_{sc} and d_M director axes with respect to the indole ring. In this case, d_{sc} is assumed to be collinear with the N_ε−H bond vector. The angle α_f defines the angle between d_M, which describes the fluctuation in orientation of the N_ε−H bond vector, and d_{sc}. For the diffusion in a cone model, the size of the cone is defined by the cone semi angle α_c, reflecting the wobbling motion of the indole ring. (B) Diagram showing the orientation of d_{sc} with respect to the orientation of the Arg side chain. Due to the rapid motions around the side chain of Arg, the NH dipolar couplings are projected along d_{sc}, which is collinear with the side chain. The angle α_f defines the angle between d_M, which describes the fluctuation in orientation of the side chain, and d_{sc}. For the diffusion in a cone model, the size of the cone is defined by the cone semi-angle α_c, and it reflects the wobbling motion of d_{sc} director axis. (C) Diagram showing the orientation of d_{sc} with respect to the helical director axis d_H. In this case, the angle Ψ is the tilt angle of the helix and ϑ is the angle between d_{sc} and d_H.

provides a viable means for determining side-chain orientation of protein embedded in lipid bilayers.

While the exact orientation of an amino acid side chain is difficult to determine due to its motional flexibility, as shown in Figure S4, our approach provides a means of correlating its dynamics and orientation based on the observed dipolar coupling values. The orientations of Trp and Arg side chains determined from this study are consistent with values reported in the literature. For example, a solid-state NMR study reported ~52° for the orientation of the N_ε−H bond vector of a Trp residue of a fd coat protein in magnetically aligned filamentous bacteriophage particles.[14] Another study on gramicidin estimated this angle to be between 40 and 60°.[15] To the best of our knowledge, no specific orientational information on the Arg side chain has been reported so far in the literature. However, the order parameter obtained in our studies is consistent with reported values ($0.2 \le S_{SC} \le 0.3$) for an antimicrobial peptide embedded in lipid bilayers.[17] Based on its location in the amino acid sequence of the mutant Cyt-b_5 and the measured order parameter, the Arg residue (observed in Figure 2) is likely to reside in the phospholipid glycerol backbone region of the lipid bilayer. Furthermore, due to the positive charge of the guanidine group in the Arg side chain, it will preferentially binds to the negatively charged phosphate headgroup of the lipid.[17] As a result, Arg side-chain motion is considerably hindered, as reflected in their relatively large NH dipolar couplings (0.77, 1.13, and 1.22 kHz) from three different NH groups (Table 1). Therefore, such information on side-chain dynamics can provide valuable insights into the topology of a membrane protein embedded in lipid bilayers.

Interestingly, the role of Arg in a membrane protein is a subject of constant debate.[18] Arg residues form an essential part of the voltage sensor domain of potassium channels, enzymes, and also other cell-membrane-permeating peptides.[18] It has also been demonstrated recently that the interaction between Arg and lipid bilayers can influence the orientation of a transmembrane helix.[18] Therefore, the ability to provide information on Arg side-chain dynamics will allow a better understanding of their role in the function of membrane proteins. Finally, the imidazole side-chain dynamics of His residues in the soluble domain are also observed using the DREPT pulse sequence. While their orientations are difficult to determine due to the motion in the soluble domain, the fact that they exhibit measurable dipolar couplings provides valuable information regarding their dynamics. Since imidazole side chains play important roles in the action of a number of enzymes, the ability to deduce their dynamics will provide insights into their role in various pH-dependent enzyme catalysis.[19]

In conclusion, we have presented a solid-state NMR technique that enables the extraction of protein side-chain dynamics in fluid lamellar-phase lipid bilayers. The NH dipolar couplings of side chains can be carefully selected through fine-tuning of the delay period in the DREPT pulse sequence. We have shown that it is possible to characterize side-chain motions by using an appropriate model. In conjunction with relaxation measurements, this can prove to be a powerful approach to determine side-chain dynamics for a variety of amino acids. Since side-chain interactions constitute the principal force dictating a protein's function, it is expected that knowledge of their dynamics will have an immense impact on our understanding of their functional role. While previous studies have utilized selective isotopic labeling approaches to measure dynamics of membrane proteins,[20−26] our approach has the unique advantage of being able to study uniformly ^{15}N- and potentially ^{15}N- and ^{13}C-labeled membrane proteins. It should be noted that the DREPT technique could also be used to characterize the dynamics of other aligned compounds, such as liquid crystalline materials, single crystals, and fibers. The ability to measure a broad range of heteronuclear dipolar couplings from DREPT experiments further advocates its usefulness in extracting residual dipolar couplings from supramolecular complexes embedded in an aligned medium.

Acknowledgment. This study was supported by research funds from NIH (GM084018 and RR023597 to A.R. and GM035533 to L.W.), CRIF-NSF, and a VA Merit Review grant to L.W. The authors thank Dr. Shivani Ahuja for help with preparation of the manuscript.

Supporting Information Available: List of abbreviations, materials and methods, pulse sequences, theory behind the DREPT pulse sequence, numerical simulation of side-chain models, and amino acid sequence of wild-type and mutant Cyt-b_5. This material is available free of charge via the Internet at http://pubs.acs.org.

References

(1) Baldwin, A. J.; Kay, L. E. *Nat. Chem. Biol.* **2009**, *5*, 808–814.
(2) McDermott, A. E. *Curr. Opin. Struct. Biol.* **2004**, *14*, 554–561.
(3) Etzkorn, M.; Kneuper, H.; Dunnwald, P.; Vijayan, V.; Kramer, J.; Griesinger, C.; Becker, S.; Unden, G.; Baldus, M. *Nat. Struct. Mol. Biol.* **2008**, *15*, 1031–1039.
(4) Ahuja, S.; Hornak, V.; Yan, E. C. Y.; Syrett, N.; Goncalves, J. A.; Hirshfeld, A.; Ziliox, M.; Sakmar, T. P.; Sheves, M.; Reeves, P. J.; Smith, S. O.; Eilers, M. *Nat. Struct. Mol. Biol.* **2009**, *16*, 168–175.
(5) Cady, S. D.; Schmidt-Rohr, K.; Wang, J.; Soto, C. S.; DeGrado, W. F.; Hong, M. *Nature* **2010**, *463*, 689–U127.
(6) Schmidt-Rohr, K.; Nanz, D.; Emsley, L.; Pines, A. *J. Phys. Chem.* **1994**, *98*, 6668–6670.
(7) Morris, G. A.; Freeman, R. *J. Am. Chem. Soc.* **1979**, *101*, 760–762. Ramamoorthy, A.; Chandrakumar, N. *J. Magn. Reson.* **1992**, *60*, 100.
(8) Dürr, U. H. N.; Waskell, L.; Ramamoorthy, A. *Biochim. Biophys. Acta* **2007**, *1768*, 3235–3259.
(9) Soong, R.; Smith, P. E. S.; Xu, J.; Yamamoto, K.; Im, S. C.; Waskell, L.; Ramamoorthy, A. *J. Am. Chem. Soc.* **2010**, *132*, 5779–5788.
(10) Dürr, U. H. N.; Yamamoto, K.; Im, S. C.; Waskell, L.; Ramamoorthy, A. *J. Am. Chem. Soc.* **2007**, *129*, 6670–6671.
(11) Burum, D.; Linder, M.; Ernst, R. R. *J. Magn. Reson.* **1981**, *44*, 173–188.
(12) Metz, G.; Xiaoling, X.; Smith, S. O. *J. Magn. Reson. A* **1994**, *110*, 219–227.
(13) Brainard, J. R.; Szabo, A. *Biochemistry* **1981**, *20*, 4618–4628.
(14) Strandberg, E.; Ozdirekcan, S.; Rijkers, D. T.; van der Wel, P. C.; Koeppe, R. E.; Liskamp, R. M.; Killian, J. A. *Biophys. J.* **2004**, *86*, 3709–3721.
(15) Cross, T. A.; Opella, S. J. *J. Am. Chem. Soc.* **1983**, *105*, 306–308.
(16) Hu, W.; Lee, K. C.; Cross, T. A. *Biochemistry* **1993**, *32*, 7035–7047.
(17) Tang, M.; Waring, A. J.; Hong, M. *Chembiochem* **2008**, *9*, 1487–1492.
(18) Vostrikov, V. V.; Hall, B. A.; Greathouse, D. V.; Koeppe, R. E.; Sansom, M. S. P. *J. Am. Chem. Soc.* **2010**, *132*, 5803–5811.
(19) Ramamoorthy, A.; Wu, C. H.; Opella, S. J. *J. Am. Chem. Soc.* **1997**, *119*, 10479–10486.
(20) Ying, W. W.; Irvine, S. E.; Beekman, R. A.; Siminovitch, D. J.; Smith, S. O. *J. Am. Chem. Soc.* **2000**, *122*, 11125–11128.
(21) Witter, R.; Nozirov, F.; Sternberg, U.; Cross, T. A.; Ulrich, A. S.; Fu, R. Q. *J. Am. Chem. Soc.* **2008**, *130*, 918–924.
(22) Vostrikov, V. V.; Hall, B. A.; Greathouse, D. V.; Koeppe, R. E.; Sansom, M. S. P. *J. Am. Chem. Soc.* **2010**, *132*, 5803–5811.
(23) Killian, J. A.; Taylor, M. J.; Koeppe, R. E. *Biochemistry* **1992**, *31*, 11283–11290.
(24) Siarheyeva, A.; Lopez, J. J.; Lehner, I.; Hellmich, U. A.; van Veen, H. W.; Glaubitz, C. *Biochemistry* **2007**, *46*, 3075–3083.
(25) Liu, W.; Crocker, E.; Siminovitch, D. J.; Smith, S. O. *Biophys. J.* **2003**, *84*, 1263–1271.
(26) Aisenbrey, C.; Prongidi-Fix, L.; Chenal, A.; Gillet, D.; Bechinger, B. *J. Am. Chem. Soc.* **2009**, *131*, 6340–6341.

JA103983F